Understanding the role of ionic flux on the polarity of the exposed surfaces of ZnO

Aditi Vijay[1#], Aritra Mukhopadhyaya[1#], Vipul Shrivastava[1#], Devanshi Bhardwaj[1], Ashok K Ganguli[2]*, Md. Ehesan Ali[1]*, Sonalika Vaidya[1]*

[1]Institute of Nano Science & Technology, Habitat Centre, Phase- X, Sector – 64, Mohali, Punjab–160062, India
[2]Department of Chemistry, Indian Institute of Technology Delhi, Hauz Khas, New Delhi-110016, India
[#]All the three authors have equal contribution

*Email: vaidyasonalika@gmail.com, svaidya@inst.ac.in

ehesan.ali@inst.ac.in, ashokganguliiitd@gmail.com

Supporting Information

Obtaining converged values for different properties for ZnO 0001 surface

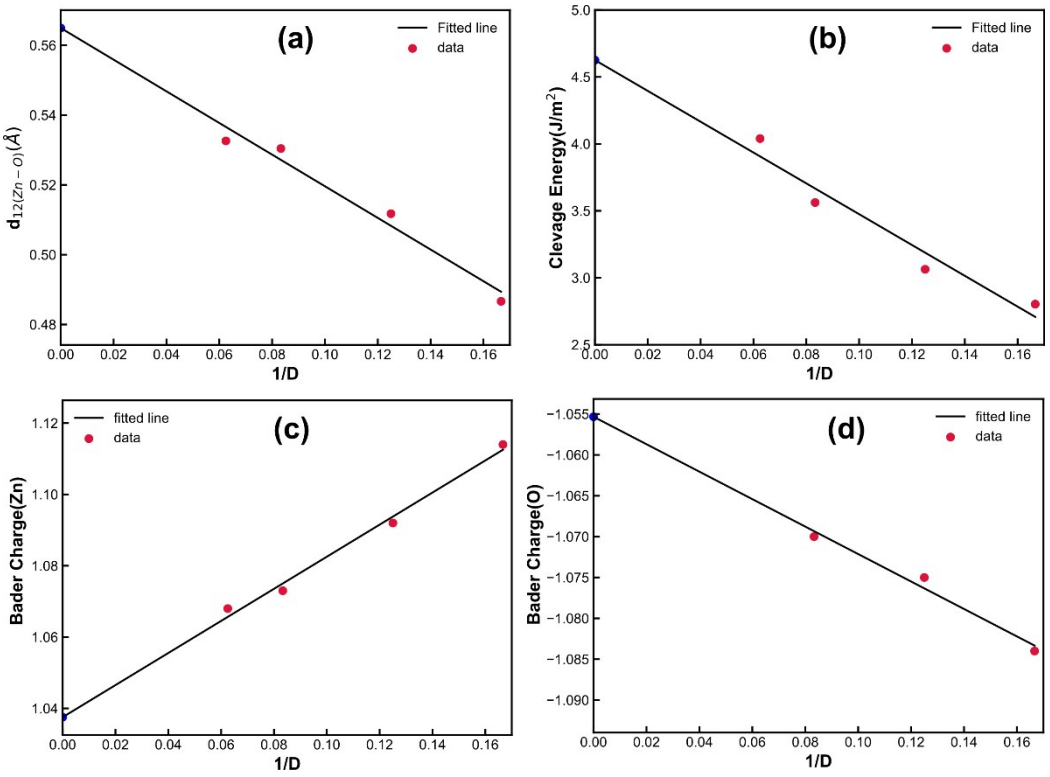

Figure S1. Calculation of several surface properties obtained from slab calculations of ZnO polar 0001 surface. The converged results are obtained by calculating the property at different slab thickness D and then extrapolating the data to 1/D→0. (a) Interlayer distance between the upper Zn and O layers. The converged value (0.56 Å) reflects an inward relaxation of the topmost Zn layer (Bulk Zn layer O layer distance is 0.59 Å). (b) Converged cleavage energy. (c) and (d) are the variation of bader population at the Zn terminal and O terminal surfaces respectively. The converged values are 1.039 and -1.055 on Zn and O. The bulk values are 1.25 and -1.30 respectively. This indicates the successful charge transfer from lower O termination to topmost Zn surface through bulk.

Optimized surface slabs obtained from VASP calculations

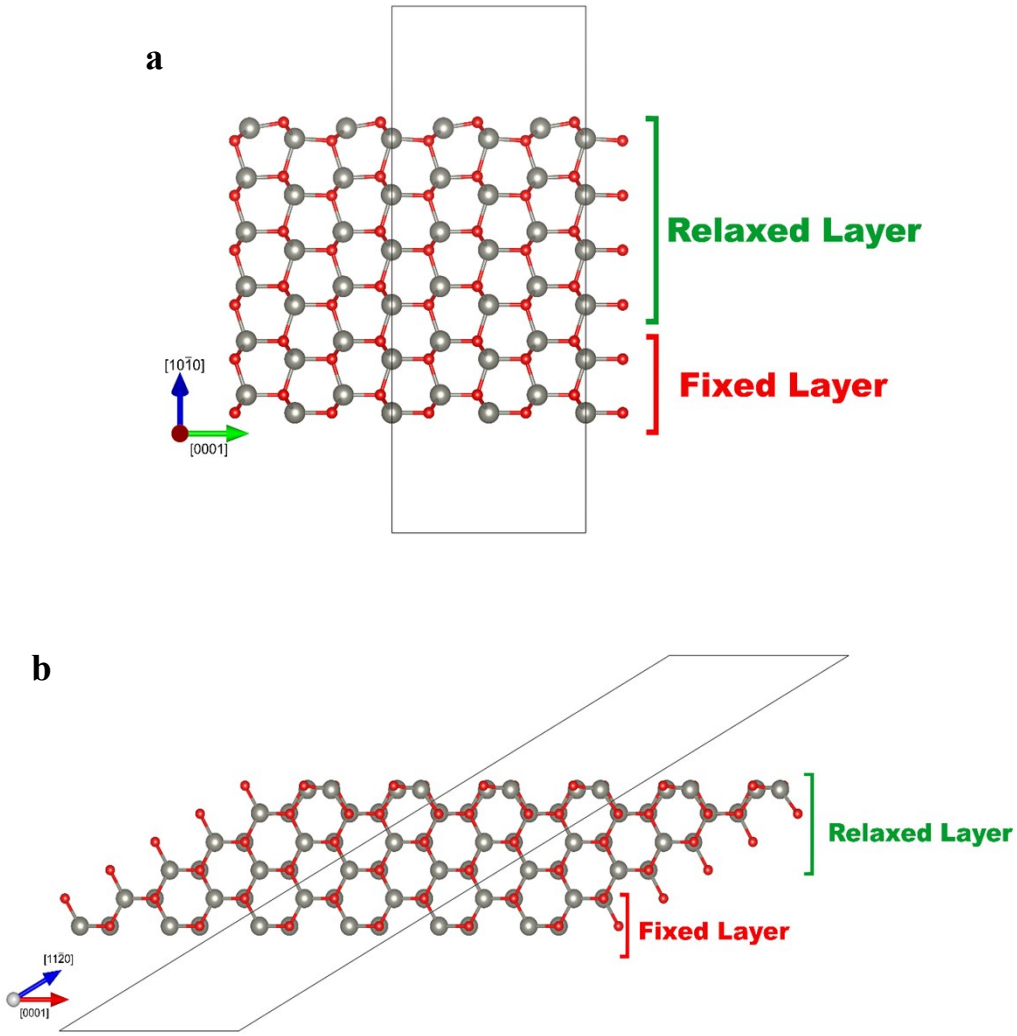

Figure S2: Relaxed $10\bar{1}0$ (a) and $11\bar{2}0$ (b) surfaces. 6 double layers of ZnO dimer was considered for both the surfaces. The lower two layers were kept fixed to their bulk position and the remaining layers were allowed to relax.

Effect of flux on non-polar surfaces

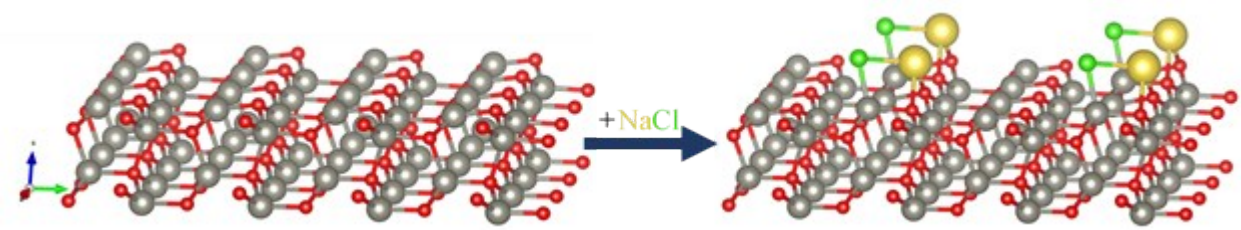

Figure S3. Accommodation of NaCl flux by relaxed ZnO $10\bar{1}0$- Surface.

Figure S3 schematically shows how the incoming flux is accommodated over the relaxed $10\bar{1}0$ surface. The Cl^- ions are accommodated by one Zn atom while the Na^+ ions are distributed by two O atoms which imply that the distribution of flux is not stoichiometric over surface atoms. The quantitative change of different structural parameters is tabulated in **Table S5**.

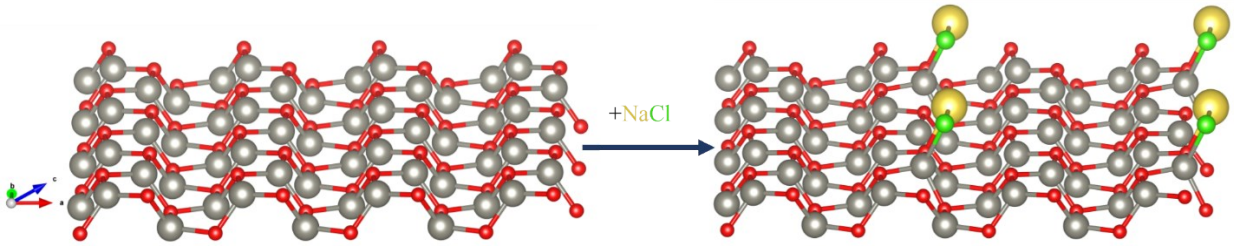

Figure S4. Accommodation of NaCl flux by relaxed ZnO $11\bar{2}0$- Surface.

Figure S4 shows the accommodation of the NaCl flux by the ZnO $11\bar{2}0$ surface. It is clear from the figure that there is no non-stoichiometric distribution of the flux over the $11\bar{2}0$ surface as it was seen in the $10\bar{1}0$ surface. Hence it can be concluded that the $11\bar{2}0$ surface is less disturbed by the ionic flux. **Table S6** quantitatively presents different structural parameters of the flux affected ZnO $11\bar{2}0$ surface. A comparison of **Table S5** and **S6** led us to conclude that $11\bar{2}0$ is less disturbed and hence more stabilized in the presence of ionic flux.

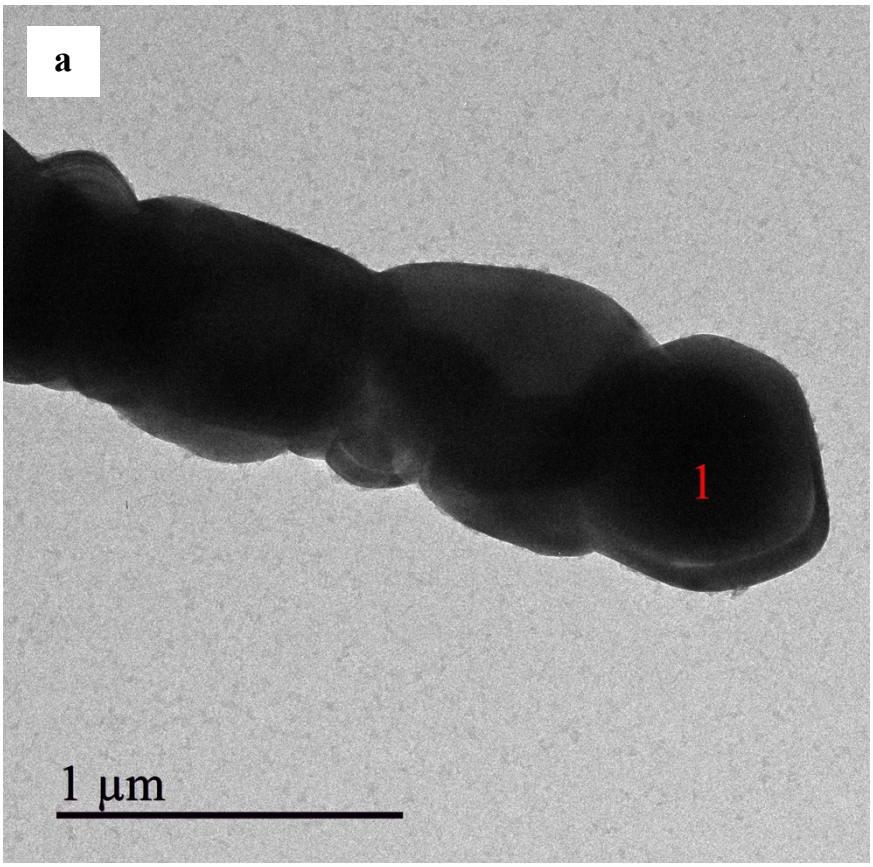
a
1
1 μm

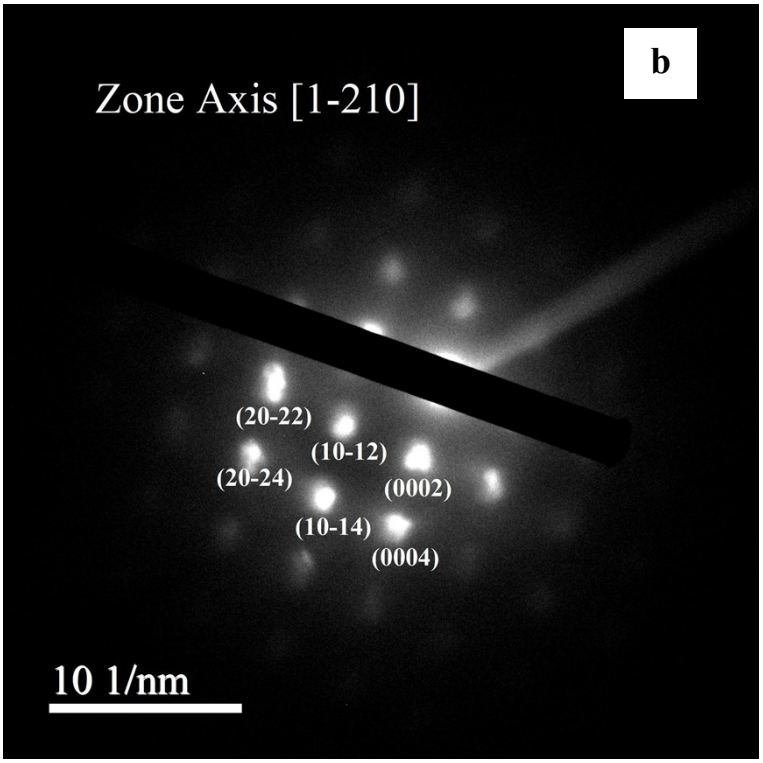
b
Zone Axis [1-210]
(20-22)
(10-12)
(20-24)
(0002)
(10-14)
(0004)
10 1/nm

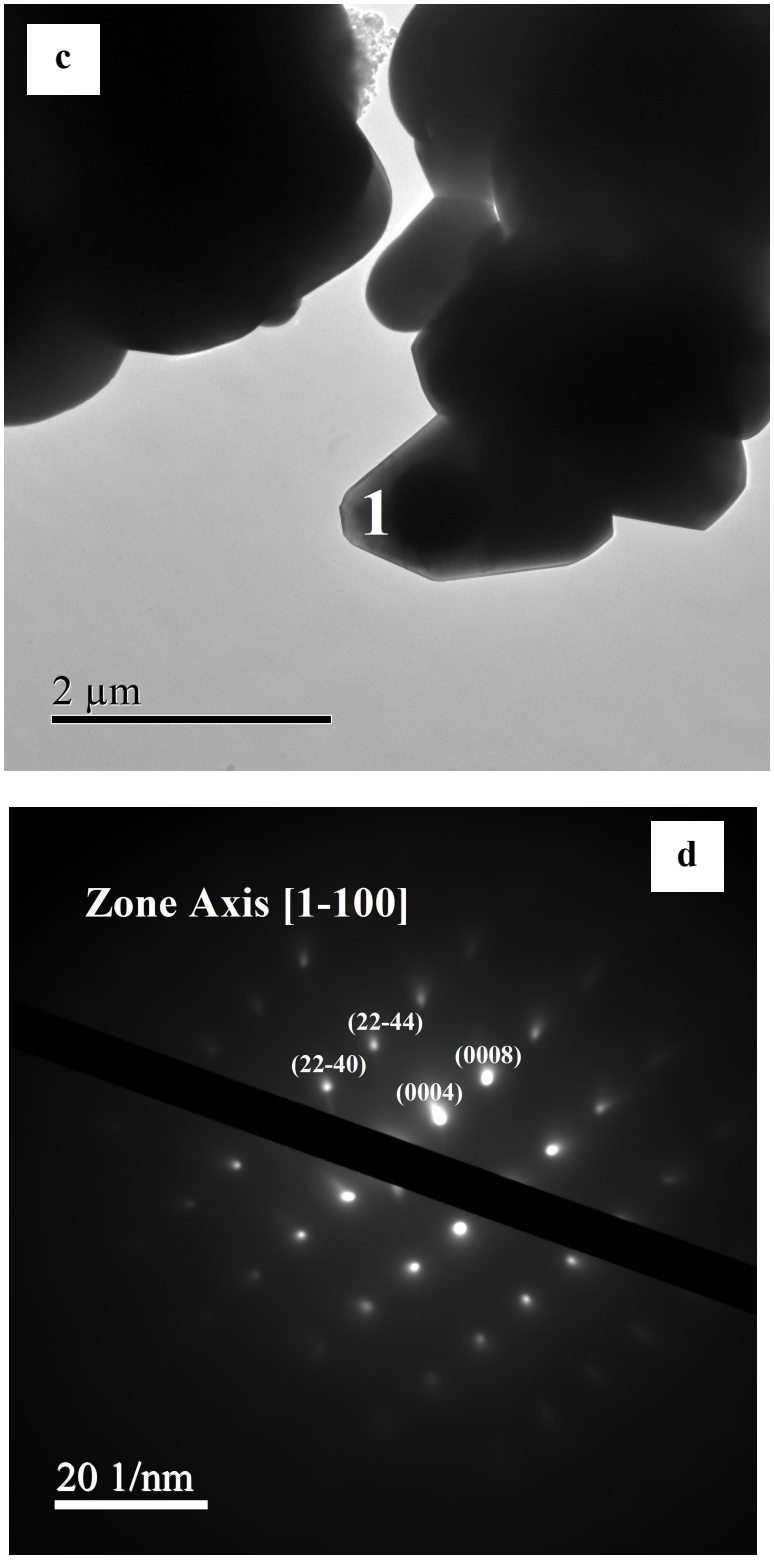

Figure S5. TEM Image of ZnO synthesized using thermal decomposition of zinc oxalate nanorods (a) in absence of flux and (c) in presence of 1:1 NaCl-KCl. Electron Diffraction pattern obtained from particle marked 1 in the corresponding TEM for ZnO obtained using thermal decomposition of zinc oxalate nanorods (b) in absence of flux and (d) in presence of 1:1 NaCl-KCl.

Particle size distribution obtained from SEM Images

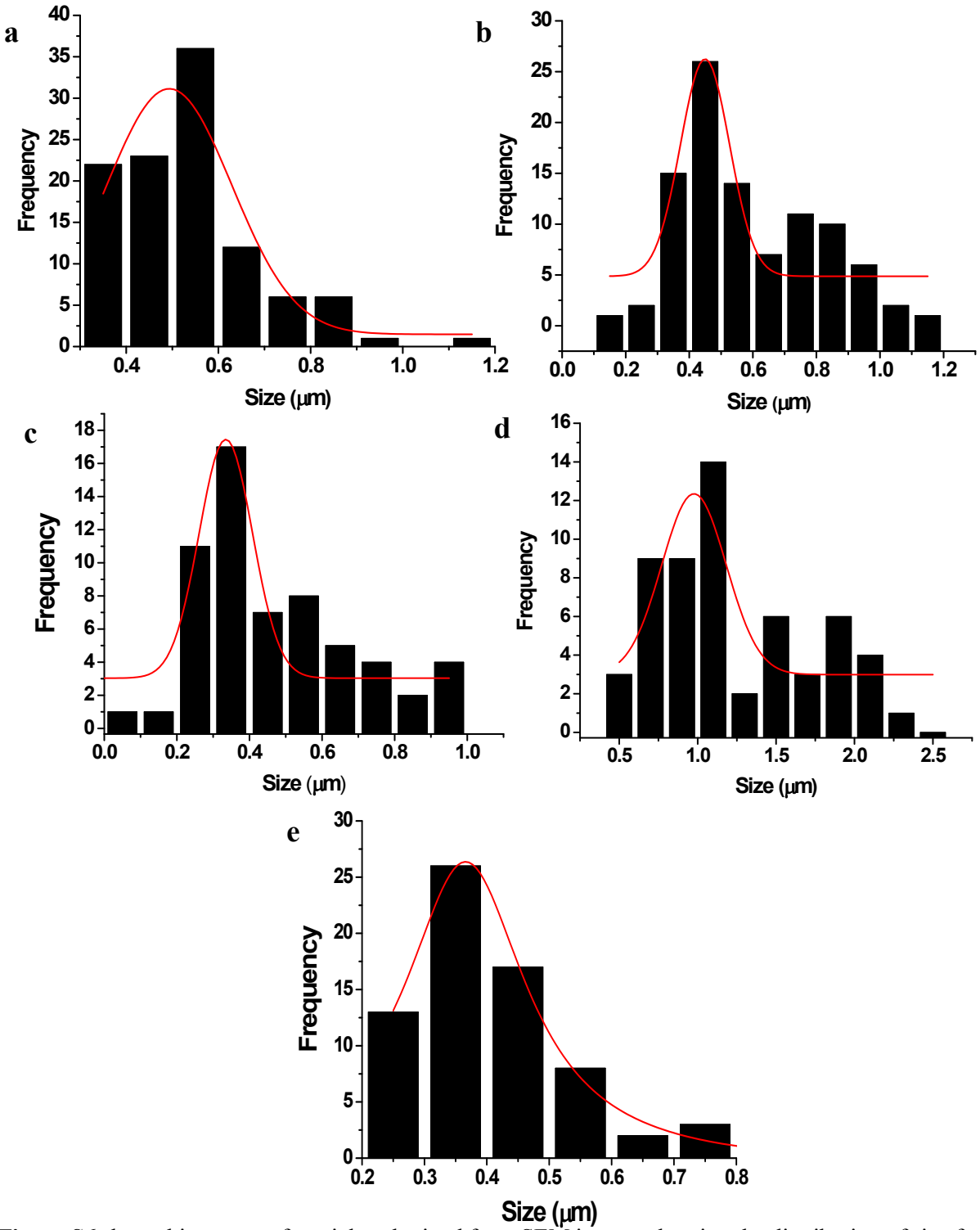

Figure S6 shows histogram of particles obtained from SEM images showing the distribution of size for ZnO obtained by decomposition of zinc oxalate (synthesized by reverse micellar route) (a) in absence of flux and presence of flux (b) NaCl, (c) KCl, (d) NaCl-KCl and (e) Na_2SO_4.

2D charge distribution analysis on ZnO surfaces.

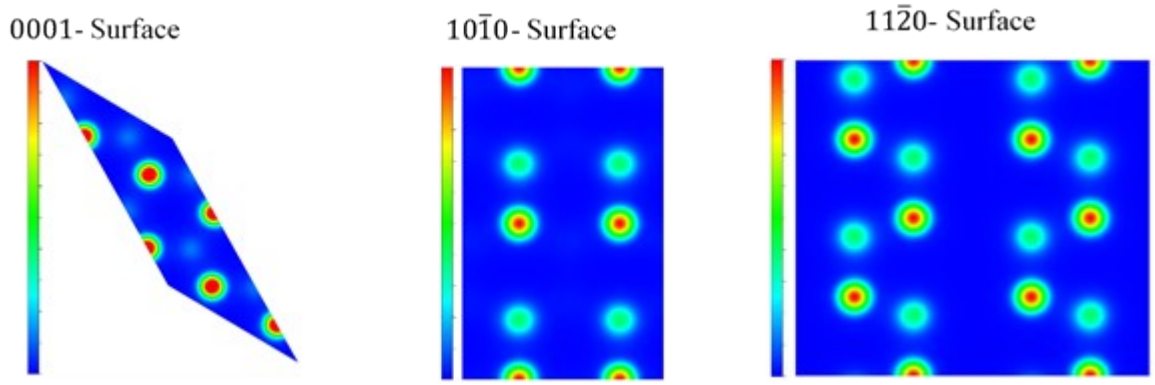

Figure S7. Electron density contour maps for different ZnO surfaces. The larger spheres represent the Zn atom while the smaller one represents O atoms.

Figure S7 shows the distribution of Zn and O charges on different ZnO surfaces. Looking at the distribution one can simply say that the 0001_- surface exerts only the Zn atoms towards the incoming flux and hence can accommodate only negative ions. While the other two surfaces are capable of accommodating both charges as they contain both Zn and O atoms. Hence it is clear that the effect of flux will be highly pronounced for the non-polar surfaces.

Estimation of electric potential and electric field for different surfaces.

To estimate the electric field intensity, we have calculated the local potential as implemented in VASP. As we are interested in the surface properties only, the local potential near the surfaces was evaluated. We have also calculated the average of the electric potential and electric field with increasing distance along the surface normal. We have used the planer average and macroscopic average schemes described by Laporte *et. al.* [42]. The analysis was performed using a python-based analysis package MacroDensty (https://github.com/WMD-group/MacroDensity). This provides a quantitative estimation of the intensity of the electric potential and electric field along the surface normal.

As the incoming flux is being accommodated at the top of the surface, the distribution of the Z-component of the electric field was mapped on a particular distance from the topmost atom of the surface. This tells us about the ease of a surface in accommodating the incoming flux. The in-plane components of the Electric field also take part in ionic interactions. Thus it is worthy to estimate the distribution of the in-plane components of the electric field over a particular surface.

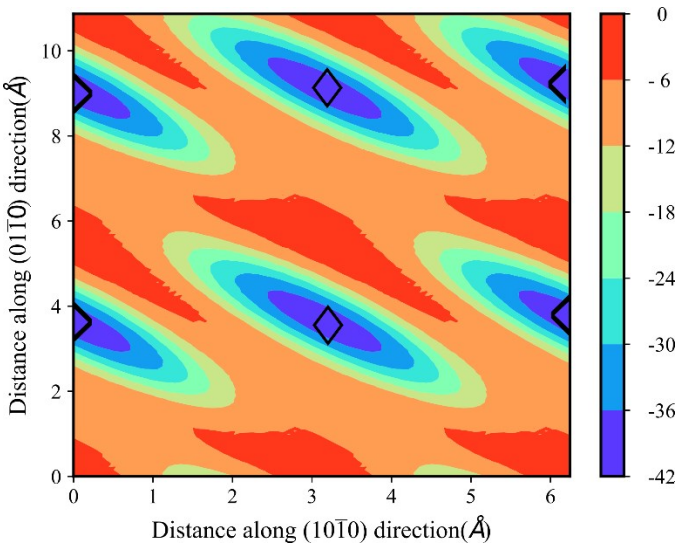

Figure S8a. Electrostatic potential contour plot for ZnO ($000\bar{1}$) surface at a distance of 0.5 Å from the topmost atom on the surface. The underlying Zn atoms are represented by the symbol ◊ while the O atom is represented by the symbol ○. The same symbols are used for the other figures and other surfaces as well.

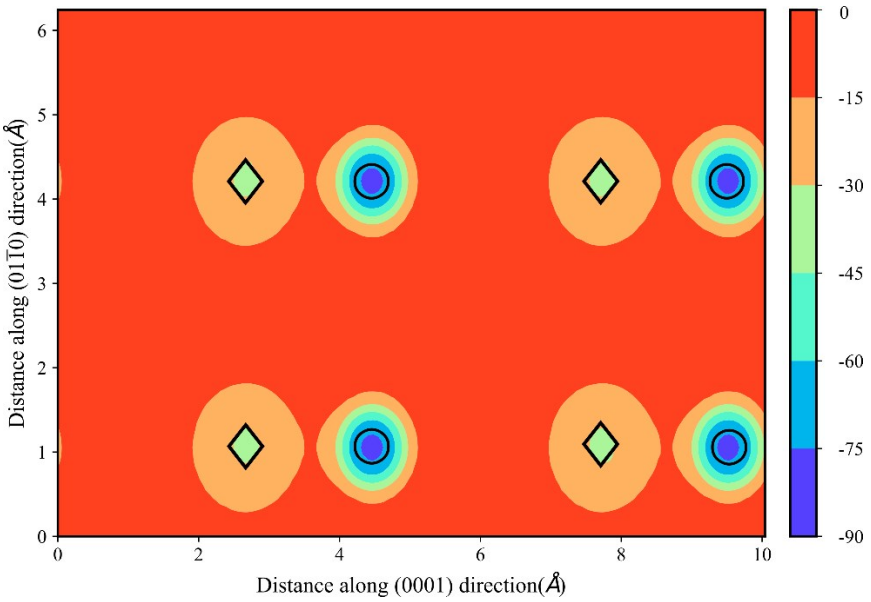

Figure S8b. Electrostatic potential contour plot for ZnO $(10\bar{1}0)$ surface at a distance of 0.5 Å from the topmost atom on the surface.

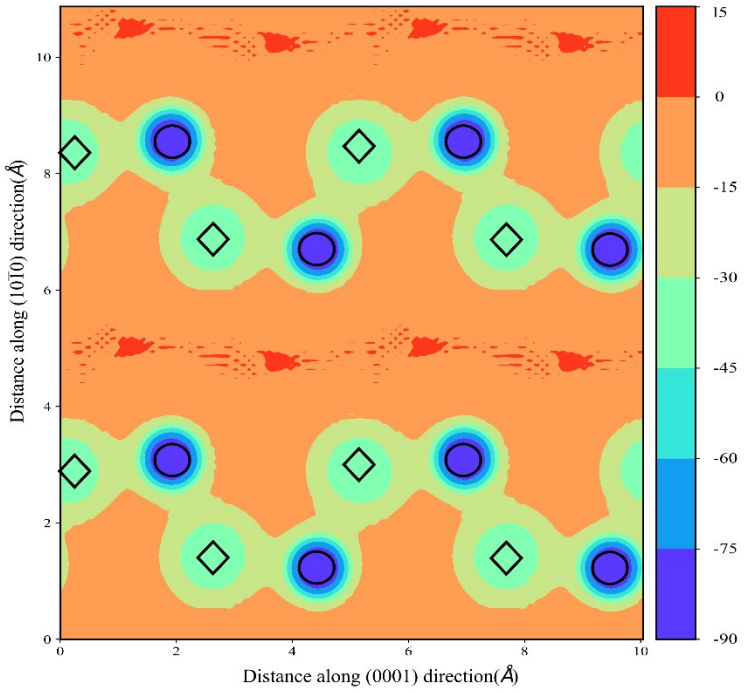

Figure S8c. Electrostatic potential contour plot for ZnO $(11\bar{2}0)$ surface at a distance of 0.5 Å from the topmost atom on the surface.

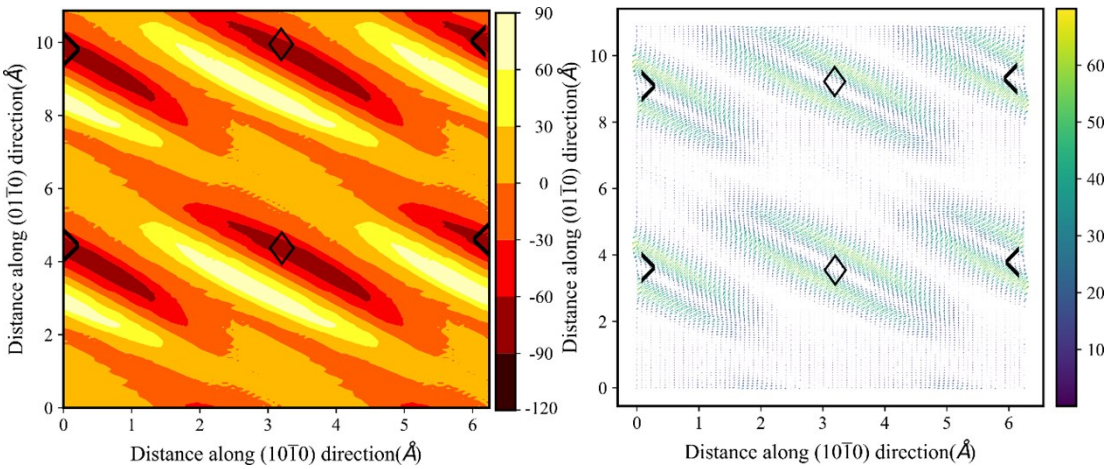

Figure S9a. Contour plot of z-component of the electric field on the XY plane for (0001) surface at the mentioned distance (Left Panel). In-plane components (E_{xy}) of the electric field (Right panel)

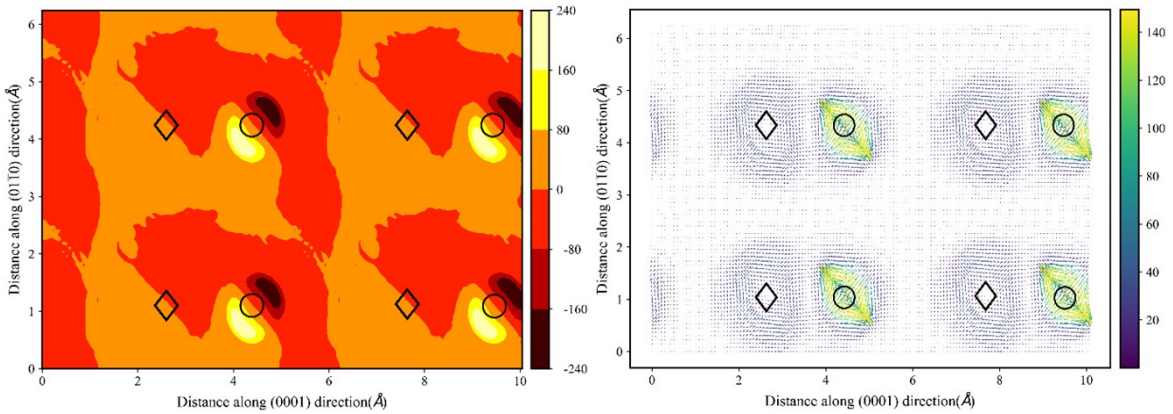

Figure S9b. Contour plot of z-component of the electric field on XY plane for $(10\bar{1}0)$ surface at the mentioned distance (Left Panel). In-plane components (E_{xy}) of the electric field (Right panel)

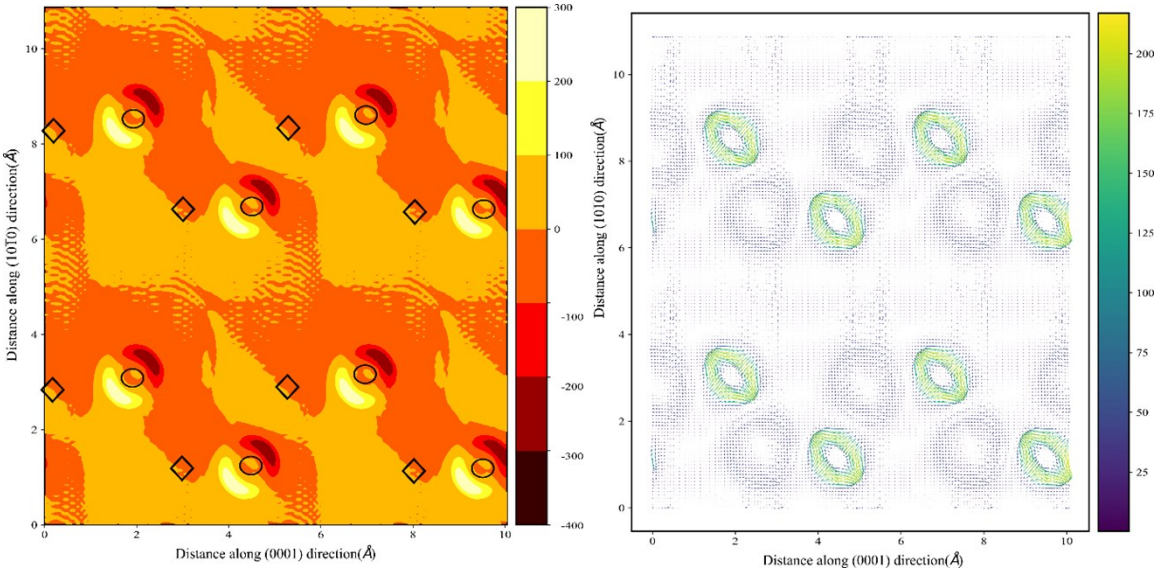

Figure S9c. Contour plot of z-component of the electric field on XY plane for ($10\bar{1}0$) surface at the mentioned distance (Left Panel). In-plane components (E_{xy}) of the electric field (right panel).

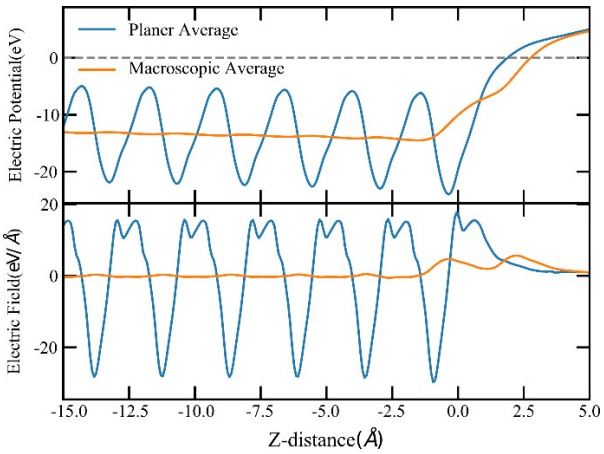

Figure S10a. Variation of average electric potential and average of the z-component of the electric field for (0001) surface along the surface normal. Z-distance 0.0 corresponds to the topmost surface atom. The negative value corresponds to the inside bulk. While positive value corresponds to a vacuum.

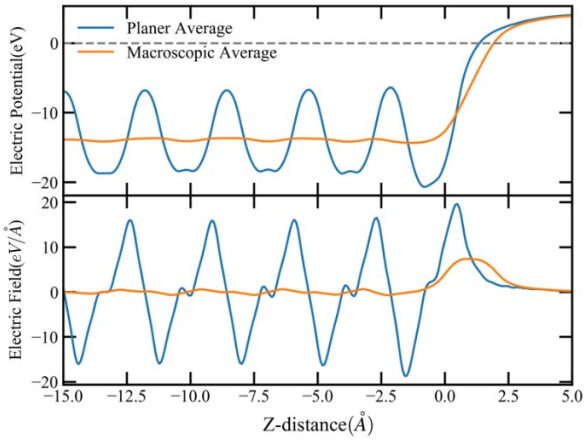

Figure S10b. Variation of average electric potential and the average of the z-component of the electric field for $(10\bar{1}0)$ surface along the surface normal.

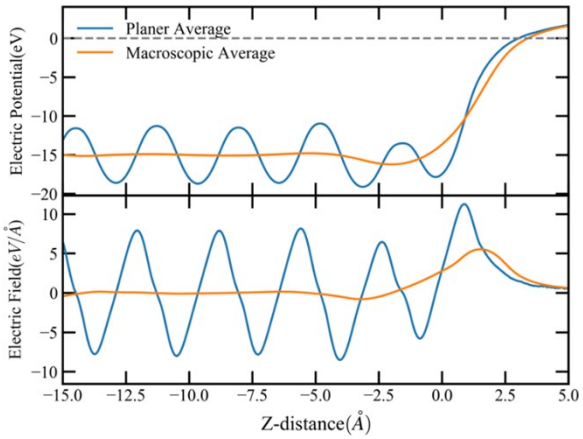

Figure S10c. Variation of average electric potential and average of the z-component of the electric field for $(11\bar{2}0)$ surface along the surface normal.

Figure S8a, S8b and S8c represents the electric potential contour map for (0001), $(10\bar{1}0)$ and $(11\bar{2}0)$ surfaces respectively. The local potential and electric fields were estimated at a distance of 0.5 Å from the topmost atom on the respective surfaces. The distribution of the electric field is presented in Figure S9 (a, b, and c). From these plots, it could be concluded that the $(10\bar{1}0)$-surface and $(11\bar{2}0)$-the surface shows a similar kind of distribution of electric field intensity at the aforementioned distance.

The variation of the average electric potential and average of the z-component of the electric field is shown in Figure S10 (a, b and c). The $(10\bar{1}0)$ surface has a higher electric field above the surface compared to $(11\bar{2}0)$ surface.

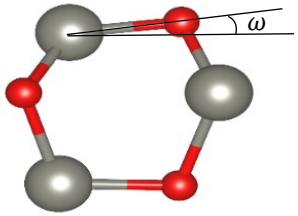

Figure S11. The tilt angle represents the angle created by the surface dimer with its bulk analogue. Thus this structural parameter is directly related to surface relaxation.

Table S1. Average Particle size obtained from Gaussian fitting of histograms of the particle size distribution for ZnO obtained by decomposition of zinc oxalate (synthesized by reverse micellar route) in presence and absence of flux.

Flux	*Average size (nm)*	*Maximum size (μm)*	*Minimum size (nm)*
No Flux	*490*	*1.15*	*350*
NaCl	*450*	*1.2*	*145*
KCl	*330*	*0.95*	*50*
NaCl-KCl	*980*	*2.3*	*500*
Na_2SO_4	*365*	*0.8*	*230*

Table S2. BET surface area for ZnO samples obtained by decomposition of zinc oxalate (synthesized via Reverse Micellar route) in presence and absence of flux

Flux	*Surface Area (m^2/g)*
No Flux	*1.5*
NaCl	*1.4*
KCl	*0.72*
NaCl-KCl	*1.2*
Na_2SO_4	*1.6*

Bader charge analysis

To evaluate the nature of interaction present between the ionic flux and ZnO dimers, we performed the Bader charge analysis for both the non-polar surfaces. From Table S3 and Table S4, the charges on the Zn and O atoms (both surface and bulk) represents the mixed ionic and covalent nature of bonding of ZnO. While the charges on Na atom and Cl atom clearly says that the flux is purely ionic in nature as there is no sign of covalent bonding.

Table S3. Bader charge analysis of the optimized flux containing ZnO $10\bar{1}0$- Surface.

Type of the atom	*Bader Charge*
Flux affected O atom	-1.342
Flux affected Zn atom	1.228
Na	0.99
Cl	-0.74
Bulk O	1.234
Bulk Zn	-1.257
Bare surface O atom	-1.2435
Bare surface Zn atom	1.2416

Table S4. Bader charge analysis of the optimized flux containing ZnO $11\bar{2}0$- Surface.

Type of the atom	***Bader Charge***
Flux affected O atom	-1.3465
Flux affected Zn atom	1.2219
Na	0.99
Cl	-0.76
Bulk O	-1.2608
Bulk Zn	1.2449
Bare surface O atom	-1.2447
Bare surface Zn atom	1.2436

Table S5. Different structural parameters in the presence and absence of NaCl flux on ZnO $10\bar{1}0$- Surface.

Structural parameter	***Value***
Flux affected surface ZnO distance	1.92 Å
Bulk ZnO distance	1.93 Å
Non-affected Surface ZnO distance	1.79 Å
Na-O distance	2.32±0.01 Å
Zn-Cl distance	2.25 Å
Tilt angle (ω) relaxed surface	9.51^0
Tilt angle (ω) for flux affected dimer (figure S3)	2.16^0/ 11.48^0

Table S6. Different structural parameters in the presence and absence of NaCl flux on ZnO $11\bar{2}0$-Surface.

Structural parameter	***Value***
Flux affected surface ZnO distance	1.95 Å
Bulk ZnO distance	1.93 Å
Non-affected Surface ZnO distance	1.81 Å
Na-O distance	2.20 Å
Zn-Cl distance	2.26 Å
Tilt angle (ω) relaxed surface	9.82^{0}
Tilt angle (ω) for flux affected dimer	4.15^{0}